# Thermal Resistor and Capacitor Parameter Identification Using Cooling Curve of IGBT Module

Jun Zhang, Xiong Du, Shuai Zheng
State Key Laboratory of Power Transmission Equipment & System Security and New Technology
Chongqing University, Chongqing, 400044, China
Email: duxiong@cqu.edu.cn

Heng-Ming Tai
Department of Electrical and Computer Engineering
University of Tulsa, Tulsa, 74104, USA

***Abstract*—In [1], we proposed a method for identifying the Cauer type thermal parameters based on the junction temperature's cooling curve of IGBT module during shutoff period. This paper utilized the identification method in [1] to realize condition monitoring. Experimental tests are performed to validate the feasibility and accuracy of this approach. Results indicate that the identified RC parameters can be used for monitoring the thermal aging of power device.**

***Keywords—Thermal parameter; condition monitoring; IGBT module***

## I. INTRODUCTION

Power converters that use insulated gate bipolar transistors (IGBT) have been widely used in various applications including wind turbines, photovoltaic generation systems, electric vehicles, railway tractions, smart grid and so on [2]. However, there is a contradiction between the service life and target lifetime of power electronic system [2]. According to an industry survey, the power device is one of the most prone to fail components in this system [3]. Therefore, there is a pressuring need to improve the reliability of power device. Main Methods for the reliability improvement of device include condition monitoring, lifetime prediction, junction temperature estimation, diagnostics and prognostics [4, 5]. These methods are closely related to the thermal parameters of Cauer network. Thus, knowing the Cauer type thermal parameters of IGBT module in the operation procedure would be beneficial to reliable operation and reliability improvement of IGBT module.

Many methods have been proposed to identify the Cauer type thermal parameters of IGBT module. One such method is to directly calculate the thermal parameter of each layer in IGBT module using the physical dimension and material properties [6-8]. The above approaches [6-8] can acquire accurate RC thermal parameters in the initial state of IGBT model, but the effect of aging process of IGBT module is not easy to be reflected. Some measurement based approaches have been put forward to consider the aging process. For example, JEDEC has released a standard to estimate the thermal parameters according to the cooling curves of junction temperature [9]. Improved methods [10, 11] calculate the thermal parameters using the network transformation algorithm introduced in [12]. These methods [9-11] can realize RC parameter estimation of Cauer network, but need to heat the module to thermal equilibrium [9-11]. Since the IGBT devices are operating in switching state and the power processed by devices are always time-varying and changing, the power loss consumed by IGBT usually is also time-varying and not constant [5]. The junction temperature always fluctuates and does not stay in a steady thermal equilibrium [5]. Therefore, above methods are not suitable for online or quasi-online application.

A few online or quasi-online thermal parameters estimation methods have been studied [13-16]. Ref [13] proposed a look up table method which reveals the relationship between the two-dimension case temperature distribution and total thermal resistance. A method to identify the increased thermal resistance by measuring the case-above-ambient temperature has been presented [14]. Ref [15] analyzed the 5$^{th}$ harmonic current of converter to obtain the increment of thermal resistance during the thermal fatigue failure process. These methods [13-15] realize the online measurement of thermal resistance, but have not taken into account the thermal capacitor. Ref [16] realizes the quasi-online thermal resistor and thermal capacitor identification under two different cooling conditions but need to measure the thermal parameters about heat sink in advance. Due to the aging effect, the same cooling condition cannot conclude the same parameter about heat sink, which reduces the method's application field.

In [1], we proposed a method for identifying the Cauer type thermal parameters only using the time constants of junction temperature cooling curves. Advantages of this approach include no need to know the loss information of IGBT module and heat the IGBT module to thermal steady state. This paper utilized the identification method in [1] to monitor the thermal aging of power device.

## II. IDENTIFICATION METHOD

### A. Thermal Network Description

Fig. 1 depicted a simple cross section of a power module which is mounted on a heat sink. The TIM is inserted between the baseplate and heat sink surface to improve physical integrity and thermal transfer [17]. According to [10], the entire thermal system can be described by a 4$^{th}$-order RC network, as

This work was supported by the National Natural Science Foundation of China under Grant 51577020.

shown in Fig. 2. In this Cauer network, $R_1$, $R_2$, $R_3$, $C_1$, $C_2$, $C_3$ are mainly related to IGBT module and TIM, $R_4$ and $C_4$ are mainly related to the heat sink [10]. The heat source or power loss is represented by $p$(t) and the ambient temperature is denoted as $T_a$. For the junction temperature $T_j$, it is very challenging to obtain it during the normal operation of converter [18]. However, when the converter is shutdown, it is relatively easy to measure the junction temperature in the shutdown procedure using the thermal sensitive electric parameter (TSEP), $V_{cesat}$, the saturation voltage of IGBT [11].

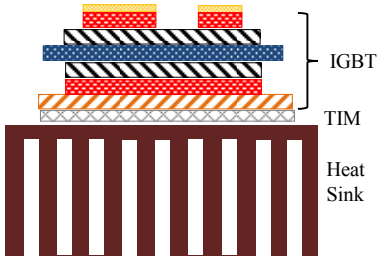


Fig. 1. Cross section of a power module with heat sink.

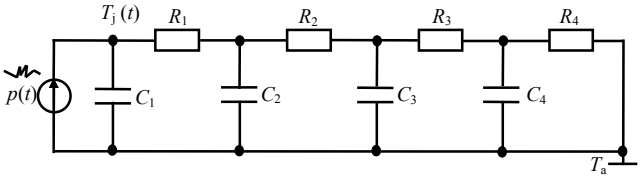


Fig. 2. 4-order RC network for entire thermal system from the chip to the ambient.

### B. *Relationship between the Time Constants of $T_{vj}(t)$ and Thermal Parameters*

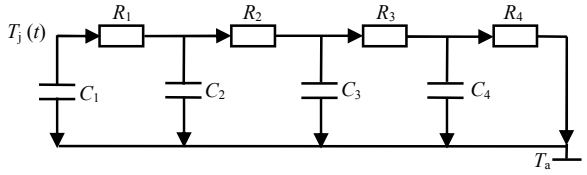


Fig. 3. $T_j(t)$ of IGBT during the shutdown process.

Since the method is performed during the IGBT shutoff period, the power loss $p$(t) is zero and the Cauer model for IGBT and heat sink becomes the thermal equivalent circuit shown in Fig. 3. Then, based on the electrical-thermal analogy and Kirchhoff's current law, the equation describing $T_{vj}$(t) can be expressed as a 4th-order homogeneous differential equation:

$$\frac{d^4T_{vj}(t)}{dt^4}+k_3\frac{d^3T_{vj}(t)}{dt^3}+k_2\frac{d^2T_{vj}(t)}{dt^2}+k_1\frac{d^1T_{vj}(t)}{dt^1}+k_0T_{vj}(t)=0 \tag{1}$$

where $T_{vj}(t)$=$T_j(t)$-$T_a$, coefficients $k_0$-$k_3$ are functions of $R_1$-$R_4$, $C_1$-$C_4$. As shown in (2)

$$\begin{cases} k_0=\dfrac{1}{C_1C_2C_3C_4R_1R_2R_3R_4} \\ k_1=\dfrac{C_1+C_2+C_3+C_4}{C_1C_2C_3C_4R_1R_2R_3}+\dfrac{C_1R_1+(C_1+C_2)R_2+(C_1+C_2+C_3)R_3}{C_1C_2C_3C_4R_1R_2R_3R_4} \\ k_2=\dfrac{C_1C_2R_1+C_3(C_1R_1+(C_1+C_2)R_2)}{C_1C_2C_3C_4R_1R_2R_3} \\ \quad+\dfrac{C_4(C_1R_1+(C_1+C_2)R_2+(C_1+C_2+C_3)R_3)}{C_1C_2C_3C_4R_1R_2R_3} \\ \quad+\dfrac{C_1C_2R_1R_2+(C_1C_2R_1+C_3(C_1R_1+(C_1+C_2)R_2))R_3}{C_1C_2C_3C_4R_1R_2R_3R_4} \\ k_3=\dfrac{C_1C_2C_3R_1R_2+C_4(C_1C_2R_1(R_2+R_3)+C_2C_3R_2R_3}{C_1C_2C_3C_4R_1R_2R_3} \\ \quad+\dfrac{C_1C_3R_3(R_2+R_1))}{C_1C_2C_3C_4R_1R_2R_3}+\dfrac{C_1C_2C_3R_1R_2R_3}{C_1C_2C_3C_4R_1R_2R_3R_4} \end{cases} \tag{2}$$

For (1), the general solution can be expressed as (3)

$$T_{vj}(t)=\alpha_1e^{-\frac{t}{\tau_1}}+\alpha_2e^{-\frac{t}{\tau_2}}+\alpha_3e^{-\frac{t}{\tau_3}}+\alpha_4e^{-\frac{t}{\tau_4}} \tag{3}$$

In (3), the solution coefficients $\alpha_i$ are related to the RC parameters and the initial voltage of each capacitor. The time constants $\tau_i$ are solely related to the RC parameters, and have the following relationships with coefficients $k_0$~$k_3$.

$$\begin{cases} k_0=\dfrac{1}{\tau_1\cdot\tau_2\cdot\tau_3\cdot\tau_4} \\ k_1=\dfrac{1}{\tau_1\cdot\tau_2\cdot\tau_3}+\dfrac{1}{\tau_1\cdot\tau_2\cdot\tau_4}+\dfrac{1}{\tau_1\cdot\tau_3\cdot\tau_4}+\dfrac{1}{\tau_2\cdot\tau_3\cdot\tau_4} \\ k_2=\dfrac{1}{\tau_1\cdot\tau_2}+\dfrac{1}{\tau_1\cdot\tau_3}+\dfrac{1}{\tau_1\cdot\tau_4}+\dfrac{1}{\tau_2\cdot\tau_3}+\dfrac{1}{\tau_2\cdot\tau_4}+\dfrac{1}{\tau_3\cdot\tau_4} \\ k_3=\dfrac{1}{\tau_1}+\dfrac{1}{\tau_2}+\dfrac{1}{\tau_3}+\dfrac{1}{\tau_4} \end{cases} \tag{4}$$

Then combining equations (2) and (4), the relationship between RC parameters and time constants can be obtained. If the cooling curve of $T_{vj}$(t) can be recorded, the time constants can be obtained by curve fitting the expression (3). Therefore, the time constants can be rated as known qualities. However, there are eight RC thermal parameters, $R_1$-$R_4$ and $C_1$-$C_4$, and only four equations are available. Thus one junction temperature cooling curve is not sufficient to estimate the RC parameters.

### C. *Additional Two Cooling Conditions*

It can be seen from Fig. 4 that $R_4$ and $C_4$ are related to the physical characteristic of the heat sink. Such as by regulating the fan speed of heat sink, the thermal characteristic of heat sink changes [19]. Under this circumstance, values of $R_4$ and $C_4$ also changes, but not the other six RC parameters. If we change the cooling condition twice, eight new equations can be obtained, except that $R_4$, $C_4$ are changed to $R'_4$, $C'_4$ and $R''_4$, $C''_4$.

Then we have twelve equations and twelve variables, and all the remaining RC parameters identification can be found with three junction temperature cooling curves.

## III. Parameter Estimation

### A. Experimental Setup

In order to verify the thermal parameter identification method, an experimental platform is constructed, as shown in Fig. 4. The device under test (DUT) is the Fuji IGBT 2MBI75VA17050 (open capsule module). The junction temperature $T_j(t)$ is measured by collecting the saturation voltage $V_{cesat}$ at low current (100mA in the test) with DAQ while the ambient temperature $T_a$ is measured by a T-type thermocouple.

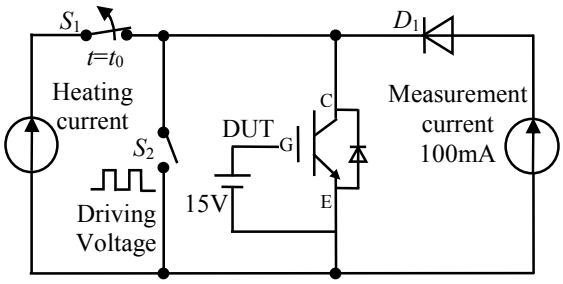


Fig. 4. Circuit for thermal parameters estimation

The procedure of the test is described in the following. First, $S_1$ is switched on and the heating current (50A) is injected into the DUT and $S_2$. The DUT is always on while the $S_2$ operates in switching state to make the junction temperature of DUT fluctuate. The control signals of $S_1$ and $S_2$ are sent by DSP. Then, after a period of heat-up, $S_1$ and $S_2$ are switched off and only the measurement current (100mA) flows through the DUT. The diode $D_1$ is used to prevent the heating current from flowing into the 100mA current source. The saturation voltage $V_{cesat}$ at low current is recorded by the DAQ. The data acquisition starts after IGBT shutoff and continues until IGBT temperature is down to the ambient temperature. Above procedure is performed at three different cooling conditions, which are denoted by FS1, FS2 and FS3.

Fig. 5 shows the junction temperature during the heating period at cooling condition FS1 which is measured by the IR camera (Optris LTF-CF2). It is observed from Fig. 5 that the DUT is in thermal non-steady state. Similar results are also obtained at cooling condition FS2 and FS3.

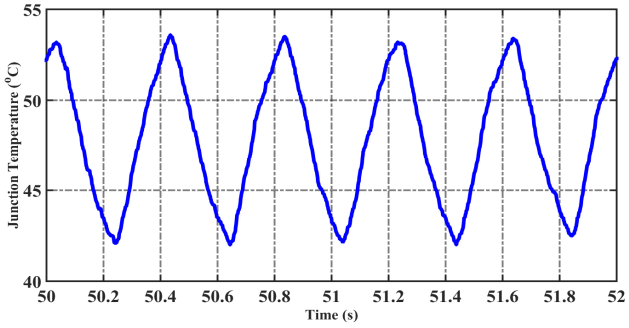


Fig. 5. Junction tmperatures measured by IR camera during the heating period at cooling condition FS1

### B. Experimental Results

Fig. 6 shows the measured curve of $T_{vj}(t)$ at cooling condition FS1 which is the junction temperature minus ambient temperature. Similar results are also obtained at cooling condition FS2 and FS3. Then the time constants at three different cooling conditions can be obtained by curving fitting these waveforms of $T_{vj}(t)$ using the expression (3). Corresponding fitted results are given in Tab. I.

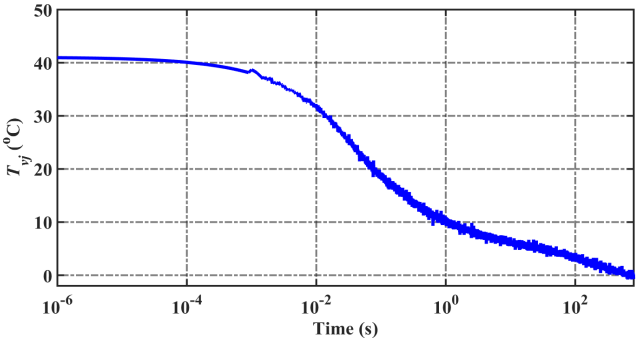


Fig. 6. $T_{vj}(t)$ waveforms of Fuji module at cooling condition FS1

TABLE I. Results of Time Constants at Different Cooling Conditions

| Cooling Conditions | Time Constants (s) | | | |
|---|---|---|---|---|
| | $\tau_1$ | $\tau_2$ | $\tau_3$ | $\tau_4$ |
| FS1 | 0.0175 | 0.1683 | 2.2509 | 172.653 |
| FS2 | 0.0175 | 0.1683 | 2.2459 | 146.000 |
| FS3 | 0.0175 | 0.1683 | 2.2419 | 104.196 |

Since we have obtained the time constants in three cooling conditions, substituting these time constants into equations about RC parameters and time constants yields the RC parameters, as shown in Tab. II.

TABLE II. Results of Identified Thermal Parameters

| Thermal Resistance (K/W) | $R_1$ | $R_2$ | $R_3$ | $R_4$ | $R'_4$ | $R''_4$ |
|---|---|---|---|---|---|---|
| | 0.213 | 0.133 | 0.080 | 0.151 | 0.138 | 0.104 |
| **Thermal Capacitance (J/K)** | $C_1$ | $C_2$ | $C_3$ | $C_4$ | $C'_4$ | $C''_4$ |
| | 0.089 | 1.236 | 27.39 | 1111 | 1025 | 969.2 |

### C. Accuracy Validation

In order to verify the accuracy of identified results, the junction temperatures measured by IR camera and that estimated based on the identified parameters are compared. The experimental platform is the same as described in Section III-A. The estimated junction temperature is obtained from Simulink calculation using the identified parameters. Fig. 7 shows the comparison results with different heating pulses at cooling condition FS1. It is observed from Fig. 7 that the

junction temperatures obtained using the estimated thermal parameters are in close agreement with that from measurement. Similar results are also obtained at cooling condition FS2 and FS3.

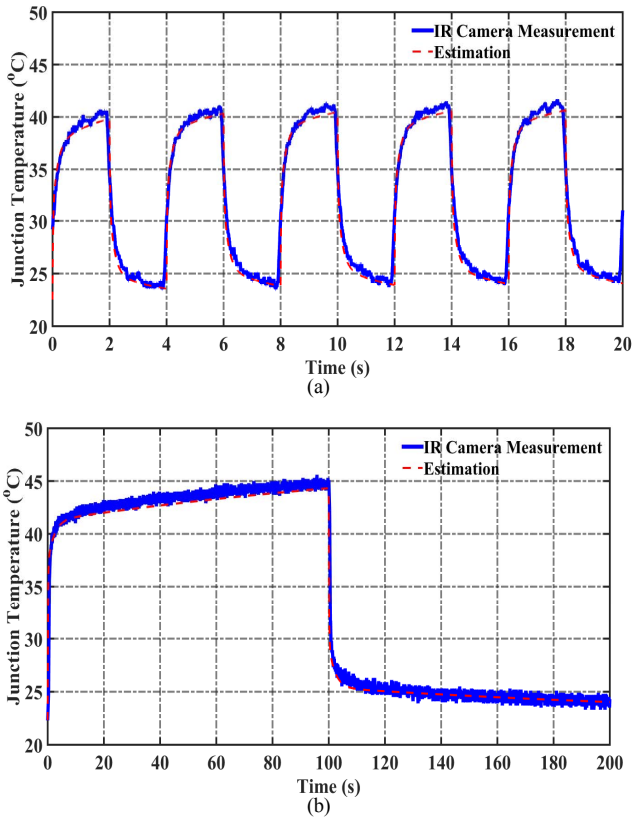


Fig. 7. The estimated and measured junction temperatures at cooling condition FS1 (a) 2-seconds heating pulse (b) 100-seconds heating pulse.

## IV. Condition Monitoring

The identified method can be used for monitoring the thermal aging of IGBT module whose directly performance is the increase of total thermal resistance [15]. According to the [21], we can simulate the "aged" module by removing the thermal grease. Similar to above test procedures in Section III-A, the identified parameters of "aged" module are shown in Tab. III. It can be seen from Tab. III that the aging affects the thermal resistance $R_3$ and $C_3$ more than other parameters. This can be attributed to the increase of void between the base plate and the heat sink.

TABLE III. Comparsion of Identified Parameters Between Aged and Healthy Modules

| Thermal Parameters | Aged | Healthy |
|---|---|---|
| $R_1$(K/W) | 0.212 | 0.213 |
| $R_2$(K/W) | 0.135 | 0.133 |
| $R_3$(K/W) | **0.261** | **0.080** |
| $R_4$(K/W) | 0.146 | 0.151 |
| $R'_4$(K/W) | 0.139 | 0.138 |
| $R''_4$(K/W) | 0.108 | 0.104 |
| $C_1$(K/W) | 0.089 | 0.089 |
| $C_2$(K/W) | 1.262 | 1.236 |
| $C_3$(K/W) | 16.48 | 27.39 |
| $C_4$(K/W) | 1151 | 1111 |
| $C'_4$(K/W) | 1015 | 1025 |
| $C''_4$(K/W) | 934.8 | 969.2 |

Also for validation of results accuracy, the junction temperatures measured by IR camera and that estimated using identified parameters are compared. The test results of "aged" module at cooling condition FS1 are given in Fig. 8. It can be seen from Fig. 8 that the estimated results match well with the measured junction temperatures, which proves that our identified parameters are accurate. Also, close examination of Fig. 7 and Fig. 8 show that the junction temperatures of the "aged" module are higher than that of the "healthy" module ("healthy" module means it inserts the thermal grease between device and heat sink). This may be due to the removal of thermal grease for the "aged" module. Similar results are obtained at cooling condition FS2 and FS3.

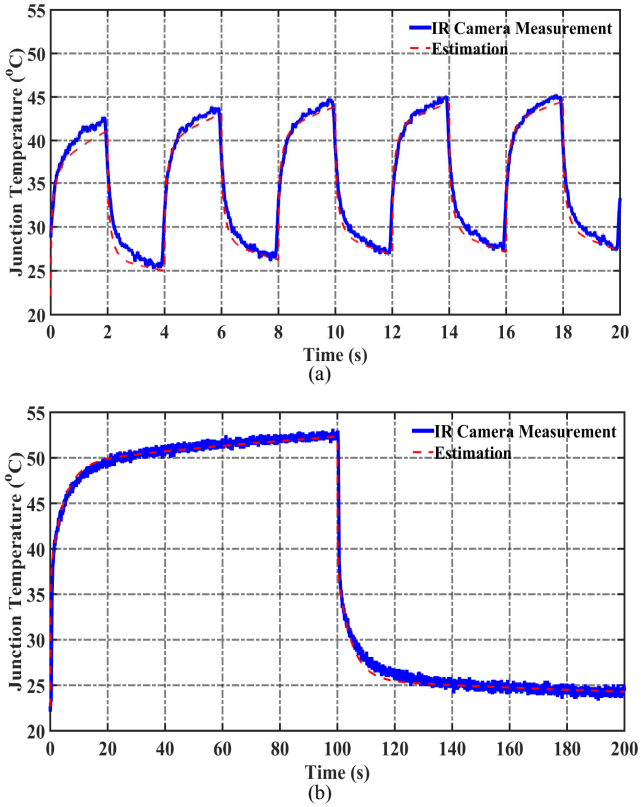

Fig. 8. The estimated and measured junction temperatures at cooling condition FS1 (a) 2-seconds heating pulse (b) 100-seconds heating pulse. (aged module)

## V. CONCLUSIONS

In [1], we presented a method to identify the RC parameters of Cauer-network during IGBT shutoff. Advantages of this method include no need to know the power loss information of IGBT and the IGBT module does not need to be heated up to thermal steady-state for accurate parameter estimation. This paper utilized the identification method in [1] to realize condition monitoring. Experimental tests have demonstrated the feasibility and accuracy of this approach. Results indicate that the identified RC parameters can be used for monitoring the thermal aging of power device.

## REFERENCES


[1] T. Li, X. Du, C. Zeng, P. Sun and H. M. Tai, "A quasi-online method of thermal network parameter identification for IGBT modules," *2016 IEEE Energy Conversion Congress and Exposition (ECCE)*, Milwaukee, WI, 2016, pp. 1-6.

[2] H. Wang et al., "Transitioning to Physics-of-Failure as a Reliability Driver in Power Electronics," *IEEE J. Emerg. Sel. Topics Power Electron.*, vol. 2, no. 1, pp. 97-114, Mar. 2014.

[3] S. Yang, A. Bryant, P. Mawby, D. Xiang, L. Ran, and P. Tavner, "An industry-based survey of reliability in power electronic converters," *IEEE Trans. Ind. Appl.,* vol. 47, no. 3, pp. 1141–1151, Feb. 2011.

[4] U.-M. Choi, F. Blaabjerg, and K.-B. Lee, "Study and handling methods of power IGBT module failures in power electronic converter systems," *IEEE Trans*. *Power Electron*., vol. 30, no. 5, pp. 2517-2533, May 2015.

[5] S. Yang *et al.*, "Condition monitoring for device reliability in power electronic converters: a review," *IEEE Trans*. *Power Electron*., vol. 25, no. 11, pp. 2734-2752, Nov. 2010.

[6] Z. Wang, and W. Qiao, "A physics-based Improved cauer-type thermal equivalent circuit for IGBT modules," *IEEE Trans*. *Power Electron*., vol. 31, no. 10, pp. 6781-6786, Oct. 2016.

[7] C. Batard, N. Ginot, and J. Antonios, "Lumped dynamic electrothermal model of IGBT module of inverters," *IEEE Trans. Compon. Packag. Manuf. Technol.*, vol. 5, no. 3, pp. 355-364, Mar. 2015.

[8] S. Bouguezzi, M.Ayadi, and M. Ghariani, "Developing a simplified analytical thermal model of multi-chip power module," *Microelectron. Reliab.*, vol. 66, pp. 64-77, Oct. 2016.

[9] Transient Dual Interface Test Method for the Measurement of the Thermal Resistance Junction to Case of Semiconductor Devices with Heat Flow Through a Single Path, JEDEC Standard 51-14, 2010.

[10] A. Hensler, M. Thoben, J. Lutz, and M. Thoben, "Thermal impedance monitoring during power cycling tests," in *Proc. PCIM Europe, Nuremberg, Germany*, 2011, pp.241-246.

[11] A. Aliyu, and A. Castellazzi, "Prognostic system for power modules in converter systems using structure function," *IEEE Trans*. *Power Electron*., vol. PP, no. 99, pp. 1-11, 2017.

[12] Y. C. Gerstenmaier, W. Kiffe, and G. Wachutka, "Combination of thermal subsystems by use of rapid circuit transformation and extended two-port theory," *Microelectron. Reliab.*, vol. 40, no. 1, pp. 26-34, Jan. 2009.

[13] Z. Wang, B. Tian, W. Qiao, and L. Qu, "Real-time aging monitoring for IGBT modules using case temperature," *IEEE Trans*. *Ind*. *Elec*., vol. 63, no. 2, pp. 1168-1178, Nov. 2015.

[14] D. Xiang et al., "Monitoring solder fatigue in a power module using case-above-ambient temperature rise," *IEEE Trans. Ind. Appl.*, vol. 47, no. 6, pp. 2578-2591, Nov.-Dec. 2011.

[15] D. Xiang et al., "Condition monitoring power module solder fatigue using inverter harmonic identification," *IEEE Trans. Power. Electron.*, vol. 27, no. 1, pp. 235-247, Jan. 2012.

[16] X. Du, T. Li, J. Zhang, H. M. Tai, P. Sun and L. Zhou, "Thermal network parameter identification of IGBT module based on the cooling curve of junction temperature," *2016 IEEE Applied Power Electronics Conference and Exposition (APEC)*, Long Beach, CA, 2016, pp. 2992-2997.

[17] B. Ji et al., "In Situ Diagnostics and Prognostics of Solder Fatigue in IGBT Modules for Electric Vehicle Drives," *IEEE Trans. Power. Electron.*, vol. 30, no. 3, pp. 1535-1543, Mar. 2015.

[18] M. A. Eleffendi, and C. M. Johnson, "Application of Kalman filter to estimate junction temperature in IGBT power modules," *IEEE Trans. Power Electron.*, vol. 31, no. 2, pp. 1576-1587, Feb. 2016.

[19] G. C. James, V. Pickert, and M. Cade, "A thermal model for a multichip device with changing cooling conditions," in *Proc. 4th IET Conf. Power Electronics, Machines & Drives*, Apr. 2008, pp. 310–314.

[20] Semiconductor devices – Discrete devices – Part 9: Insulated-gate bipolar transistors (IGBTs), IEC Standard 60747-9, 2007.

[21] H. Chen, B. Ji, P. Ghimire, V. Pickert and W. Cao, "Real-Time temperature estimation for power MOSFETs considering thermal aging effects," *IEEE Trans. Device Mater. Reliab.*, vol. 14, no. 1, pp. 220-228, Mar. 2014.